 DOI:10.30420/566414066

Improved MRAS-based Speed Sensorless Control of PMSM Considering Inverter Nonlinearity

Longbing Song[1], Lie Xu[1], Weidong He[1], Yanjie Han[1], Shaoyi Sun[1]
[1] Department of Electrical Engineering Tsinghua University, Beijing 100084, China

Corresponding author: Weidong He, hwd21@mails.tsinghua.edu.cn
Speaker: Longbing Song, slb22@mails.tsinghua.edu.cn

Abstract

This article analyzes the shortcomings of the speed sensorless control strategy based on traditional MRAS methods. It does not take into account the voltage difference caused by the nonlinear characteristics of the inverter and the current difference caused by sampling time delay. This leads to errors in speed and angle estimation. To address this issue, this article analyzes the sources of nonlinear voltage errors in inverters, derives voltage compensation formulas, and applies them to the MRAS model. In addition, to address the issue of sampling delay, this paper proposes an improved MRAS structure that ensures consistent sampling time for voltage and current. Moreover, voltage feedforward is added in the speed estimation process to compensate for the impact of sampling current lag. This article measured some nonlinear parameters of the inverter through experiments, and finally verified the feasibility of this method through simulation.

Key words: DTP-PMSM, MRAS, inverter nonlinearity, sampling delay

1 Introduction

At present, permanent magnet synchronous motor (PMSM) is widely used in electric propulsion system. Usually, PMSM need to be equipped with speed sensors to provide real-time feedback of the rotational speed, but this increases the cost and reduces the reliability[1]. Therefore, speed sensor-less technology has received much attention in electric airplane systems.Model Reference Adaptive System (MRAS) is a common method for speed sensorless control[2]. However, as the control performance requirements increase[3], velocity sensorless methods have shown some drawbacks, and the MRAS method is not an exception.

In the MRAS method, in order to obtain an accurate speed estimation, the stator current and the motor terminal voltage need to be sampled. Generally, the motor terminal voltage is replaced by the reference voltage of the inverter. Therefore, the voltage and current cannot be sampled simultaneously, and the current signal will have hysteresis, which affects the dynamic characteristics of the speed estimation. In addition, the influence of the inverter is not considered in the derivation of the adaptive law. As a matter of fact, the switching characteristics of the inverter and the dead band etc. will have an impact. The nonlinear error of the inverter introduces distortion of the motor stator voltage, thereby reducing the estimation performance. Therefore, it is necessary to include the inverter in the derivation of the equation when deriving the adaptive law. Scholars have conducted detailed research on the dead zone and compensation mechanism of inverters[4]. Reference [6] proposes a simple scheme based solely on current control to accurately identify the nonlinear effects of inverters. The work of this article is based on this idea. The method of using an estimated voltage error lookup table (LUT) is used to address the impact of inverter nonlinearity on speed sensorless systems. Reduced the impact of inverter nonlinearity on sensorless control algorithms[6]. The impact of inverter nonlinearity on speed sensorless control is greater at low speeds. Reference [7] corrected the nonlinear voltage distortion by self adjusting the inverter model, achieving high dynamic performance at extremely low speeds.

2 Mathmatical Model of DTP-PMSM and the method of MRAS

2.1 Mathmatical Model of DTP-PMSM

Dual three-phase permanent magnet synchronous motor(DTP-PMSM) is widely used in aeronautical electric propulsion systems.After a simple Park transformation, we can get the new voltage-current equation as,

$$\begin{cases} u_d = r_s i_d + L_d \dfrac{di_d}{dt} - \omega L_q i_q \\ u_q = r_s i_q + L_q \dfrac{di_q}{dt} + \omega (L_d i_d + \psi_f) \end{cases} \tag{1}$$

Simultaneously, the electromagnetic torque can be calculated as,

$$T_e = 3p[(L_d - L_q) i_d i_q + i_q \psi_f] \tag{2}$$

The mechanical equations of the motor are as follows,

$$T_e = J \cdot \frac{d\omega_m}{dt} + B \cdot \omega_m + T_L \tag{3}$$

The general equation for the motor can be obtained from equations (1-3) as,

$$\frac{d}{dt}\begin{bmatrix} i_d \\ i_q \\ \omega_e \end{bmatrix} = \begin{bmatrix} -\frac{R_s}{L_d} \cdot i_d + \omega_e \cdot \frac{L_q}{L_d} \cdot i_q \\ -\frac{R_s}{L_q} \cdot i_q - \omega_e \cdot \frac{L_d}{L_q} \cdot i_d - \frac{\psi_f}{L_q} \cdot \omega_e \\ \frac{3p^2}{J} \cdot (L_d - L_q) \cdot i_d i_q + \frac{3p^2}{J} \cdot \psi_f \cdot i_q - \frac{B}{J} \cdot \omega_e - \frac{p}{J} \cdot T_L \end{bmatrix} + \begin{bmatrix} \frac{1}{L_d} & 0 \\ 0 & \frac{1}{L_q} \\ 0 & 0 \end{bmatrix} \cdot \begin{bmatrix} V_d \\ V_q \end{bmatrix} \tag{4}$$

Equation 4 can be abbreviated as,

$$\dot{x} = f(x) + A \cdot u \tag{5}$$

It is clear that this is a nonlinear equation with nonlinear terms $\omega_e i_d$, $\omega_e i_q$ and $i_d i_q$. In order to decouple the electrical quantities i_d and i_q from the mechanical quantity ω_e , the speed ω_e is usually considered as a variable that changes slowly compared to the electrical quantities. This needs special attention during MRAS design, especially when the nonlinearity of the inverter is also taken into account.

2.2 The traditional method of MRAS

MRAS consists of three main components: reference model, adjustable model, and adaptive law[8]. The control block diagram of the three components is shown in Fig. 1, where the reference model acts as the controlled object, which is a DTP-PMSM. The adjustable model is the mathematical representation of the controlled object, and within the adjustable model, there is unknown rotor position information to be estimated. By adjusting the adjustable model based on the output error between the reference model and the adjustable model, the adjustable model is aligned with the reference model's output. We can get the motor speed information by this method.

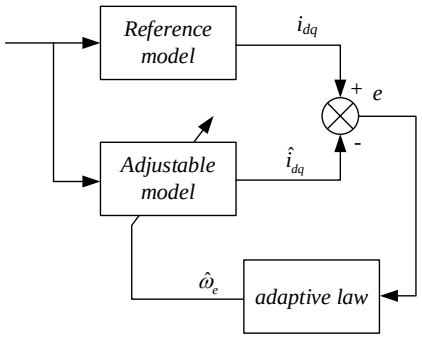

Fig. 1. The principle of MRAS

Equation 6 for the estimation of the rotational speed is derived using Popov's stability, and the derivation is omitted in this document.

$$\hat{\omega}_e = (k_p + \frac{k_i}{s})[i_d \hat{i}_q \frac{L_q}{L_d} - \hat{i}_d i_q \frac{L_d}{L_q} - \frac{\psi_f}{L_q}(i_q - \hat{i}_q) + (\frac{L_d}{L_q} - \frac{L_q}{L_d})\hat{i}_d \hat{i}_q] \tag{6}$$

Integrating the rotational speed estimation results gives the rotor position estimation results as,

$$\hat{\theta}_e = \int \hat{\omega}_e dt + \theta_e(0) \tag{7}$$

The block diagram of speed sensorless vector control based on MRAS method is shown in Fig. 2.

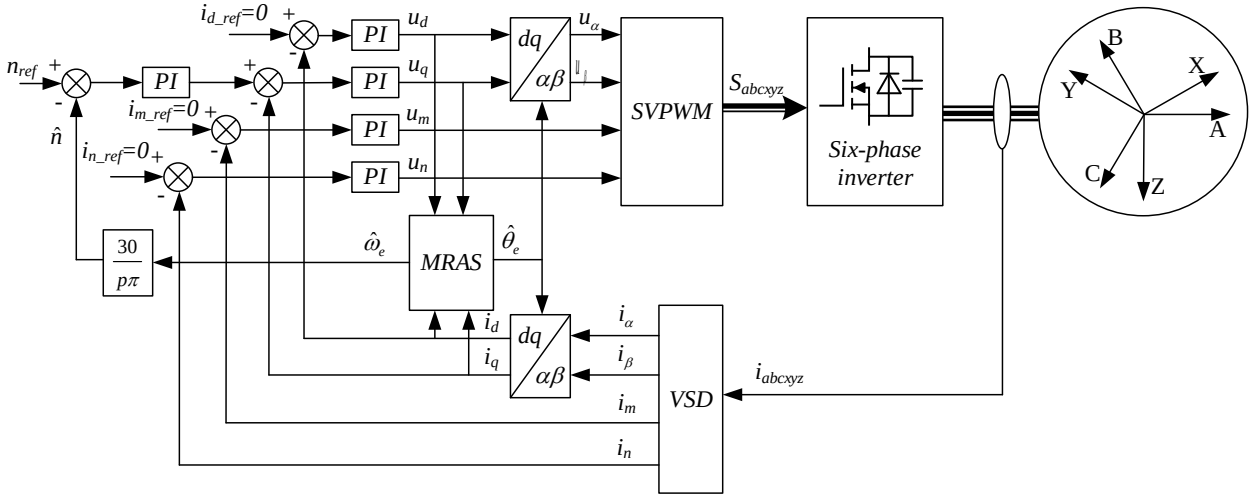

Fig. 2. Block diagram of speed sensorless vector control based on MRAS method

 DOI:10.30420/566414066

3 Compensation of Inverter Nonlinearity Voltage

3.1 Analysis of Inverter Nonlinearity Voltage Error

3.1.1 The impact of the switching process

A leg of the inverter is analyzed as shown in Fig.3. The presence of inverter dead time causes a voltage deviation between the inverter reference voltage and the inverter output voltage. Furthermore, considering the presence of parasitic capacitance in the switching transistor, the output voltage variation of the inverter cannot be instantaneous.

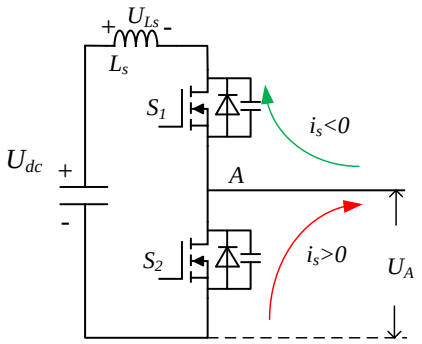

Fig. 3. A leg of an inverter

The switching influence of the inverter is related to the direction of the current, and Fig. 4 illustrates this pattern. If $i_s>0$, when $t<t_0+t_{off}$, S_2 conducts and current flows through S_2. At this point, $U_A=0$. When $t=t_0+t_{off}$, S_2 turns off. During this process, the current is flowed through the diode in S_2. So, $U_A=0$. When $t=t_1+ t_{on}$, S_1 turns to conduct, the diode in S_2 is disconnected and $U_A=U_{dc}$. When $t=t_2+ t_{off}$, S_1 turns off and U_A starts to fall and $U_A=0$. If $i_s<0$, when $t<t_0+t_{off}$, S_2 conducts and current flows through S_2. At this point, $U_A=0$. When $t=t_0+t_{off}$, S_2 starts to turn off and U_A starts to fall and $U_A=U_{dc}$. When $t=t_2+t_{off}$, S_1 begins to turn off. During this process, the current is flowed through the diode in S_1. So, $U_A=U_{dc}$. When $t=t_3+t_{on}$, S_2 turns to conduct, the diode in S_1 is disconnected and $U_A=0$.

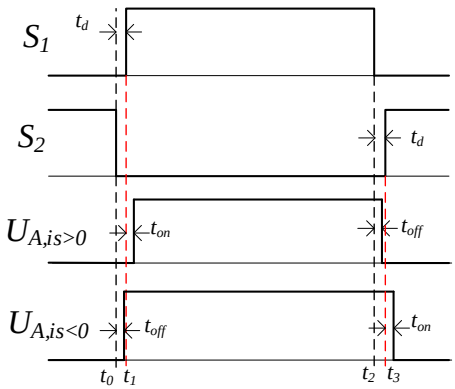

Fig. 4. The switching influence of the inverter

Therefore, the error time is,

$$t_{error} = (t_d + t_{on} - t_{off})sign(i_s) \tag{8}$$

The actual voltage considering the impact of the switching process is,

$$U_{A\_real1} = U_{A\_ref} + \frac{t_{error}}{T_s}U_{dc} \tag{9}$$

3.1.2 The voltage drop of MOSFET and body diode

The conduction resistance of this type of SiC-MOSFET is 2.6$m\Omega$. The forward conduction voltage of the body diode is 4.65V.

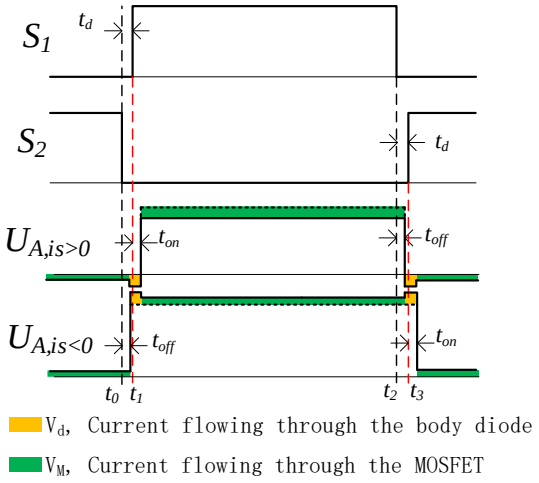

Fig. 5. The voltage drop of MOSFET and body diode

If $i_s>0$, when $t<t_0+ t_{off}$, S_2 conducts and current flows through S_2, $\Delta U_A=-V_M$. When $t= t_0+t_{off}$, S_2 turns off. During this process, the current is flowed through the diode in S_2, $\Delta U_A=-V_d$. When $t=t_1+t_{on}$, S_1 turns to conduct, $\Delta U_A=-V_M$. When $t=t_2+t_{off}$, S_1 turns off, $\Delta U_A=-V_d$. If $i_s<0$, when $t<t_0+t_{off}$, S_2 conducts and current flows through S_2, $\Delta U_A=V_M$. When $t= t_0+t_{off}$, S_2 turns off. During this process, the current is flowed through the diode in S_1, $\Delta U_A=V_d$. When $t=t_1+t_{on}$, S_1 turns to conduct, $\Delta U_A=V_M$. When $t=t_2+t_{off}$, S_1 turns off, $\Delta U_A=V_d$.

The actual voltage considering the voltage drop of MOSFET and body diode is,

$$U_{A\_real2} = U_{A\_ref} - sign(i_s)(V_M + \frac{2(t_d + t_{on} - t_{off})}{T_s}(V_d - V_M)) \tag{10}$$

3.1.3 The voltage drop of Stray inductance

There is a certain amount of stray inductance on the circuit of the inverter. During the current switching process, the changing current will generate a certain voltage drop on the stray inductance of the inverter, thereby affecting the output voltage. The stray parameters of the inverter need to be measured through a dual pulse experiment.

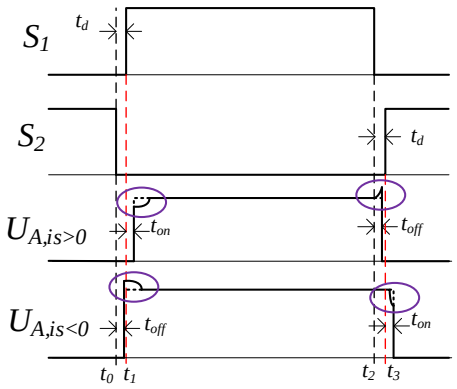

Fig. 6. The voltage drop of Stray inductance

If $i_s>0$, when $t=t_1+t_{on}$, S_1 turns to conduct, $U_{Ls}>0$. When $t=t_2+t_{off}$, S_1 turns off. The current flowing through L_s sharply decreases, so, $U_{Ls}<0$. If $i_s<0$, when $t= t_0+t_{off}$, S_2 turns off. The current flowing through L_s sharply increases and $U_{Ls}<0$. When $t=t_3+t_{on}$, S_2 turns on, $U_{Ls}>0$.

The actual voltage considering the voltage drop of MOSFET and body diode is,

$$U_{real\_3} = U_{ref} + sign(i_s)\frac{1}{T_s}\int_{I_1+I_2} U_{Ls}\cdot dt \tag{11}$$

Based on the above analysis, the actual voltage considering the Inverter nonlinearity is,

$$\begin{aligned} U_{A\_real} &= U_{A\_ref} + \frac{t_{error}}{T_s}U_{dc} + sign(i_s)\frac{1}{T_s}\int_{I_1+I_2} U_{Ls}\cdot dt \\ &- sign(i_s)(V_M + \frac{2(t_d + t_{on} - t_{off})}{T_s}(V_d - V_M)) \end{aligned} \tag{12}$$

3.2 Compensation of Sampling delay

In the speed sensorless algorithm, the voltage signal is the reference voltage, while the current signal is the actual collected signal. Therefore, there is a delay of one sampling period in the current signal. The speed estimation result can be written as,

$$\omega = \Lambda(u_{dq,k}, i_{dq,k-1}) \tag{13}$$

Obviously, such an estimation result cannot reflect dynamic changes in a timely manner. Specifically, mismatched voltage and current values may result in significant errors in the estimation results.

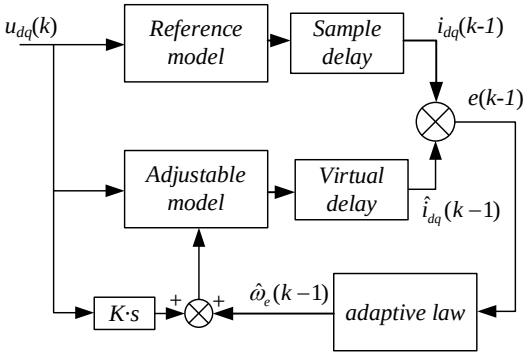

Fig. 7. Improved MRAS considering sampling delay

In order to maintain consistency between the current generated by the adjustable model and the reference model, the output results of the adjustable model are delayed for one sampling period before participating in the operation. But at this point, the estimated speed also delays by one sampling cycle. Therefore, consider introducing the latest u_{dq} in differential form into the estimation model as a feedforward to cope with significant speed adjustments.

3.3 MRAS Model considering Inverter Nonlinearity

As shown in Fig. 8, nonlinear compensation and sampling delay compensation are added to the original MRAS block diagram.

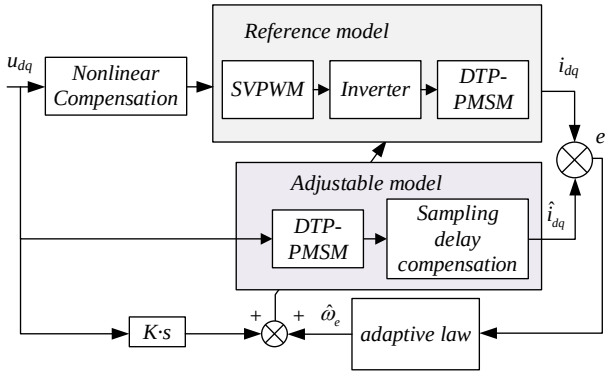

Fig. 8. The principle of improved MRAS

In the traditional MRAS design, the adjustable model is selected as the voltage-current model of the motor. As a matter of fact, this method has some errors, especially those caused by the nonlinear effects of the inverter. Therefore, it is necessary to select the adjustable model for the real reference model.

Two compensations were added to the model. The nonlinear compensation is used to compensate the voltage deviation due to inverter nonlinearity. The sampling delay compensation is used to compensate for current differences due to sampling time.

4 Simulation and Experiment

4.1 Parameter measurement

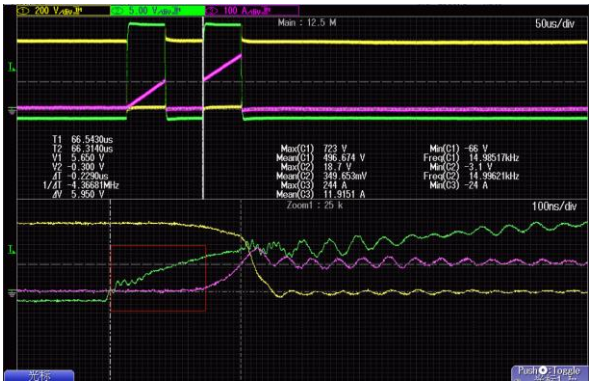

Fig. 9. Test of t_{on}

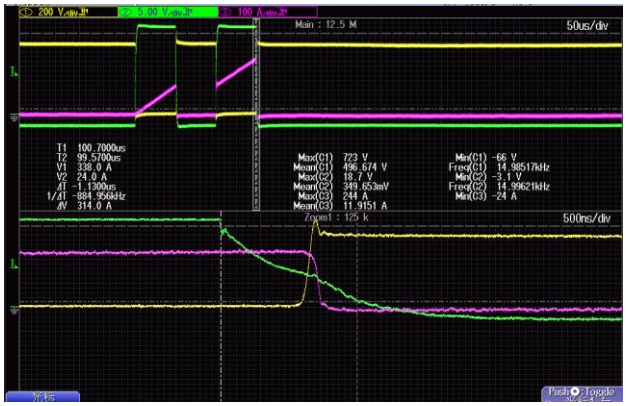

Fig. 10. Test of t_{off}

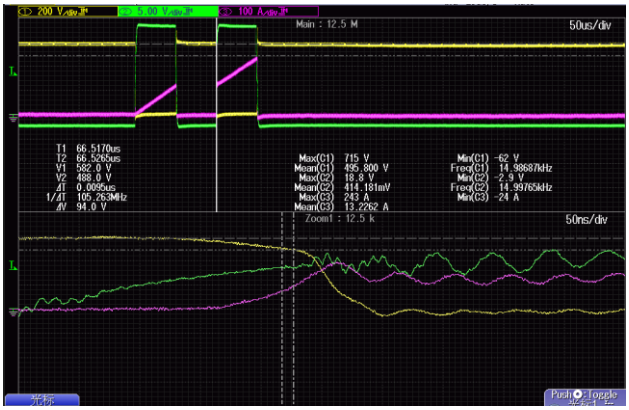

Fig. 11. Test of L_s

Conduct a dual pulse experiment on the SiC-MOSFET used in the experiment to determine the accurate t_{on} and t_{off}, determine the actual dead time, and calculate the compensation value based on this.

According to experimental measurements, t_{on}=0.169us, t_{off}=0.83us. Under the condition of 700V on the busbar, the stray inductance has a voltage drop of up to 94V.

4.2 simulation result

For the above analysis, the simulation model is built in MATLAB for simulation verification. The parameters of DTP-PMSM are shown in Table.1.

Table. 1. The Parameters of DTP-PMSM

parameter	***value***
Stator resistance/Ω	1.4
d-axis inductance/mH	7.88
q-axis inductance/mH	7.88
leakage inductance/mH	1.76
permanent magnet flux/Wb	0.68
Number of pole pairs	3

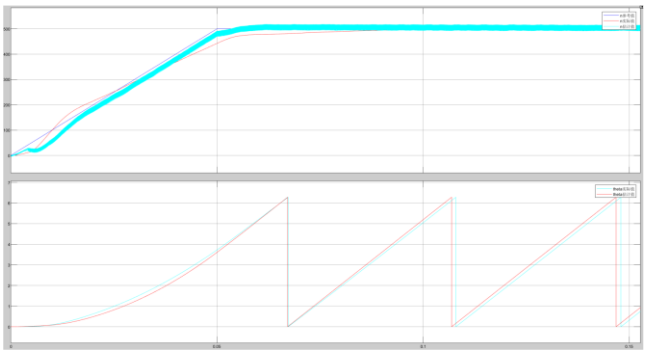

(a)Traditional MRAS

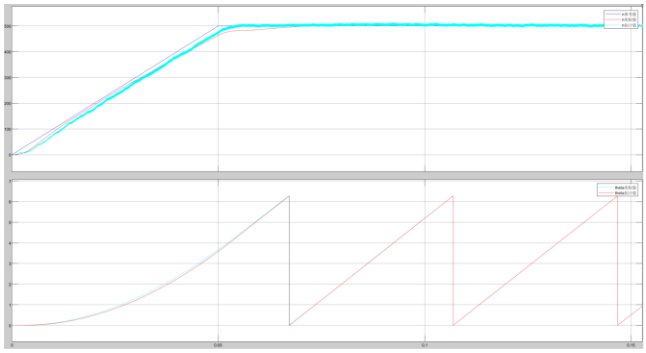

(b)Improved MRAS

Fig. 12. Comparison of MRAS before and after improvement

From the simulation results, it can be seen that after considering the nonlinear compensation of the inverter and the sampling delay compensation, the accuracy of the speed estimation value has been significantly improved, and the error in rotor position estimation has been significantly reduced.

5 Conclusion

This article compensates the MRAS model in two ways, one is inverter nonlinear compensation, which is used to compensate for voltage errors caused by inverter dead zone and voltage drop. The source of nonlinear voltage error in inverters was derived, and the formula for voltage compensation was obtained. Finally, it was added as a compensation quantity to the MRAS model, effectively ensuring the consistency between the reference voltage and the actual voltage. Another type is sampling delay compensation, which is used to compensate for the current error caused by sampling delay. Delaying the voltage so that it comes from the same sampling period as the current value effectively reduces the instability of MRAS estimation caused by voltage and current asynchrony. In addition, incorporating real-time reference voltage as a feedforward variable into speed estimation compensates for the impact of current sampling delay. Finally, the nonlinear parameters of the inverter were accurately measured through experiments, and a corresponding simulation model was established. The simulation results demonstrate the effectiveness of this

method. Moreover, the simulation results are similar to the actual experimental results.

The results of this article are applied to high-performance control of aviation electric propulsion motors. This method can effectively improve the accuracy of speed sensorless control, thereby enhancing the control accuracy of speed and torque. This is very beneficial for the application scenarios of aviation electric propulsion motors. However, this article still requires a lot of detailed argumentation and specific experiments, which will be carried out in subsequent work.

6 Acknowledgements

This work was supported by the National Key R&D Plan of China under Grant No.2022YFB4300200.

7 References

[1] S. K. Kakodia and G. Dyanamina, "Sliding Mode MRAS Observer for PMSM-fed Electric Vehicle Control using Recurrent Neural Network-Based Parallel Resistance Estimator," 2023 IEEE Transportation Electrification Conference and Expo, Asia-Pacific (ITEC Asia-Pacific), Chiang Mai, Thailand, 2023, pp. 1-6, doi: 10.1109/ITECAsia-Pacific59272.2023.10372190.

[2] A. Mishra, V. Mahajan, P. Agarwal and S. P. Srivastava, "MRAS based estimation of speed in sensorless PMSM drive," 2012 IEEE Fifth Power India Conference, Murthal, India, 2012, pp. 1-5, doi: 10.1109/PowerI.2012.6479492.

[3] H. Li, Z. Wang, C. Wen and X. Wang, "Sensorless Control of Surface-Mounted Permanent Magnet Synchronous Motor Drives Using Nonlinear Optimization," in IEEE Transactions on Power Electronics, vol. 34, no. 9, pp. 8930-8943, Sept. 2019, doi: 10.1109/TPEL.2018.2885552.

[4] J.W. Choi and S.K. Sul, “Inverter output voltage synthesis using novel dead time compensation,” IEEE Trans. Power Elctron., vol. 11, no. 2, pp. 221-227, Mar. 1996.

[5] I. R. Bojoi, E. Armando, G. Pellegrino and S. G. Rosu, "Self-commissioning of inverter nonlinear effects in AC drives," 2012 IEEE International Energy Conference and Exhibition (ENERGYCON), Florence, Italy, 2012, pp. 213-218, doi: 10.1109/EnergyCon.2012.6347755.

[6] T. Wang, B. Shi, J. Xu and C. Gerada, "Accuracy improvement of carrier signal injection sensorless control for IPMSM in consideration of inverter nonlinearity," IECON 2015 - 41st Annual Conference of the IEEE Industrial Electronics Society, Yokohama, Japan, 2015, pp. 000273-000278, doi: 10.1109/IECON.2015.7392111.

[7] J. Holtz and Juntao Quan, "Sensorless vector control of induction motors at very low speed using a nonlinear inverter model and parameter identification," in IEEE Transactions on Industry Applications, vol. 38, no. 4, pp. 1087-1095, July-Aug. 2002, doi: 10.1109/TIA.2002.800779.

[8] Y. Ouyang and Y. Dou, "Speed Sensorless Control of PMSM Based on MRAS Parameter Identification," 2018 21st International Conference on Electrical Machines and Systems (ICEMS), Jeju, Korea (South), 2018, pp. 1618-1622, doi: 10.23919/ICEMS.2018.8549314.

